Redox Regulation of RhoA

Jongyun Heo,[‡,§] Kimberly W. Raines,[‡,||] Viorel Mocanu,[‡] and Sharon L. Campbell*[,‡,||]

Department of Biochemistry and Biophysics and the Lineberger Comprehensive Cancer Center, The University of North Carolina, 530 Mary Ellen Jones Building, Chapel Hill, North Carolina 27599-7260

Received May 21, 2006; Revised Manuscript Received August 29, 2006

ABSTRACT: We have previously shown that redox agents including superoxide anion radical and nitrogen dioxide can react with GXXXXGK(S/T)C motif-containing GTPases (i.e., Rac1, Cdc42, and RhoA) to stimulate guanine nucleotide release. We now show that the reaction of RhoA with redox agents leads to different functional consequences from that of Rac1 and Cdc42 due to the presence of an additional cysteine (GXXXCGK(S/T)C) in the RhoA redox-active motif. While reaction of redox agents with RhoA stimulates guanine nucleotide dissociation, RhoA is subsequently inactivated through formation of an intramolecular disulfide that prevents guanine nucleotide binding thereby causing RhoA inactivation. Thus, redox agents may function to downregulate RhoA activity under conditions that stimulate Rac1 and Cdc42 activity. The opposing functions of these GTPases may be due in part to their differential redox regulation. In addition, the results presented herein suggest that the platinated-chemotherapeutic agent, cisplatin, which is known for targeting nucleic acids, reacts with RhoA to produce a RhoA thiol−cisplatin−thiol adduct, leading to inactivation of RhoA. Similarly, certain arsenic complexes (i.e., arsenate and arsenic trioxide) may inactivate RhoA by bridging the cysteine residues in the GXXXCGK(S/T)C motif. Thus, in addition to redox agents, platinated-chemotherapeutic agents and arsenic complexes may modulate the activity of GTPases containing the GXXXCGK(S/T)C motif (i.e., RhoA and RhoB).

Similar to Ras GTPases, Rho family GTPases regulate a host of cellular processes involved in regulation of cellular growth control, i.e., cell proliferation, apoptosis, and differentiation (*1*−*3*). However, Ras and Rho GTPases interact with distinct regulatory factors and cellular targets to mediate pathways that control these processes (*1*−*3*). Moreover, Rho GTPases regulate pathways that modulate cell morphology and motility through actin cytoskeletal rearrangements as well as oxidant production (*2*−*5*).

The activity of Rho GTPases is modulated by protein regulatory factors which control cycling between active GTP-bound and inactive GDP-bound states. For example, guanine nucleotide exchange factors (GEFs) upregulate Rho GTPase activity by facilitating exchange of bound GDP with GTP to populate the active GTP-bound state of the GTPase. Downregulation of Rho GTPase activity is achieved by GTPase-activating proteins (GAPs) and GDP dissociation inhibitors (Rho GDIs) which enhance the intrinsic GTP hydrolysis and prevent membrane association and GDP dissociation, respectively (*6*, *7*). Exchange of GDP for GTP leads to a conformational change in the GTPase that greatly enhances their affinity for downstream effectors. The interaction between the active GTP-bound GTPase and effector leads to stimulation of GTPase effector-mediated signal transduction pathways.

In addition to these protein regulatory factors, we have recently demonstrated that reactive oxygen species (ROS) and reactive nitrogen species (RNS), particularly superoxide anion radical ($O_2^{\bullet-}$) and nitrogen dioxide ($^{\bullet}NO_2$), respectively, can enhance GDP release from a subset of Rho GTPases (i.e., Cdc42, Rac1, and RhoA) and thus modulate their activity (*8*). The redox sensitivity of these Rho GTPases is due to the presence of a redox-active GXXXXGK(S/T)C motif located in the phosphoryl-binding loop (*8*). This GXXXXGK(S/T)C motif is also found in other Rho family GTPases (i.e., RhoT and TC10), several Rab GTPases as well as the Ran family GTPase, TC4. Intriguingly, a variant form of the GXXXXGK(S/T)C motif, which contains an additional cysteine (Cys^{16}, RhoA numbering) designated herein as the "GXXXCGK(S/T)C motif", is found in a subset of redox-active GTPases, including RhoA and RhoB. In RhoA, the redox-active Cys^{20} (equivalent to Rac1 Cys^{18}) is ∼3.6 and ∼10.3 Å away from Phe^{30} (equivalent to Phe^{28} in Ras and Rac1) and Cys^{16} (not present in Ras and Rac1), respectively (*9*). Although the redox architecture of RhoA (*9*) is nearly identical to that of Rac1 and Cdc42 (*10*, *11*), electronic interaction between Cys^{16} and Cys^{20} in RhoA may give rise to distinct redox properties compared to Rho GTPases containing a single cysteine within the GXXXXGK(S/T)C motif, such as Rac1 (*12*).

cis-Diamminedichloroplatinum (II) (cisplatin) is widely used in chemotherapy to target and modify nucleic acids (*13*−*16*), and is particularly effective in the treatment of testicular, ovarian, head, neck, and non-small cell lung cancer (*13*−*16*). However, cisplatin has significant toxicity and is mutagenic in cell culture and animal model systems. (*trans*-*R*,*R*)1,2-Diaminocyclohexaneoxalatoplatinum (II) (oxalipl-

* Corresponding author. E-mail: campbesl@med.unc.edu. Fax: (919) 966-2852. Tel: (919) 966-7139.

‡ Department of Biochemistry and Biophysics.

§ Current address: Department of Chemistry and Biochemistry, University of Texas at Arlington, Arlington, TX 76019.

|| Lineberger Comprehensive Cancer Center.

10.1021/bi0610101 CCC: $33.50
Published on Web 11/09/2006

atin) is a second generation platinum complex that is often effective in cisplatin-resistant cell lines and tumors and appears to be less mutagenic than cisplatin (*17*−*19*). Part of the mutagenic and toxic affects associated with these platinated-chemotherapeutic agents may result from reactivity with cellular proteins (*20*−*22*), due to their high affinity with thiols (*23*, *24*). For example, platins (i.e., cisplatin and oxaliplatin) can react and bridge vicinal protein thiols in thioredoxin reductase resulting in inactivation (*25*). Like platins, many metal complexes (i.e., arsenic and vanadium complexes), can cross-link protein bithiols (*26*−*28*). In fact, one arsenic complex, phenylarsine oxide (PAO), has been shown to cross-link the Cys^{16} and Cys^{20} thiols of RhoA, leading to RhoA inactivation (*29*). As the GXXXCGK(S/T)C motif of RhoA contains a bithiol, we postulated that platins as well as other thiol-reactive metals and their derivatives could target RhoA, resulting in alteration of RhoA-mediated signaling events.

In this study, mutagenesis, kinetic, fluorescence spectroscopy, and mass spectrometry approaches have been employed to investigate the role of reactive oxygen and nitrogen species on GXXXCGK(S/T)C motif-containing GTPases. We have also investigated the effect of various platinated-chemotherapeutic and arsenic agents on the guanine binding and exchange properties of GXXXCGK(S/T)C-motif-containing GTPases.

MATERIALS AND METHODS

Chemicals and Experimental Conditions. The typical assay buffer consists of 5 mM ammonium acetate, 5 mM $MgCl_2$, and 50 mM NaCl (pH 7.5). The metal content in the assay buffer was minimized by passing the buffer through a metal-chelating Bio-Rad Chelex-100 cation exchange column and by adding 100 μM DTPA to the buffer prior to performing the experiments (*8*, *30*). $^{\bullet}NO_2$ (99.5%) and N_2 (99.9%) gases were obtained from Aldrich. The determination of $^{\bullet}NO_2$ content (0 to $\sim$5 μM) in anaerobically sealed vials containing assay buffer has been described previously (*8*). Aquated cisplatin and oxaliplatin were employed as thiol cross-linking agents. Cisplatin was obtained from Sigma; Pt(dach)Cl_2 was provided by Dr. S. D. Wyrick (UNC). All platination reactions were carried out with aquated derivatives of the platinum complexes to facilitate their reaction with other substrates. The aquated complexes were prepared using methods described elsewhere (*31*−*33*). Fluorescence labeled mant-GDP[1] was obtained from Molecular Probes. Other chemicals used for the experiments were purchased from Sigma and Aldrich, and were of the highest grade.

Preparation of Protein Samples. Wt RhoA(1−181), RhoA F25N, RhoA C16A/F25N, RhoA C20A/F25N, wt Rac1(1−177), and wt Cdc42(1−188) proteins were expressed and purified as described previously (*8*, *34*). RhoA C16A/F25N and C20A/F25N mutants were prepared by QuikChange Site-directed Mutagenesis Kit (Stratagene). Vav2 DPC was expressed and purified as described previously (*34*). The prepared proteins were >95% pure as determined by SDS−PAGE, and the protein concentration was determined by the Bradford method (*35*). The purified Rho proteins were incubated with DTT (10 mM) for 10 min under anaerobic conditions. DTT was then removed by passing redox-active Rho protein samples through a size exclusion column (G-25, 1 × 5.0 cm) that was pre-equilibrated anaerobically with the assay buffer under anaerobic conditions.

Preparation and Quantification of Oxidized Rho Proteins. DTT-treated Rho GTPases were introduced into anaerobically sealed vials containing $^{\bullet}NO_2$ (0 to $\sim$5 μM) in assay buffer and incubated for 10 min. Ascorbate (1 mM) was then added to quench the remaining $^{\bullet}NO_2$ and radicalized protein prior to air exposure. RhoA GTPases treated with $^{\bullet}NO_2$ followed by ascorbate were applied to a size exclusion column (G-25, 1 × 5.0 cm) to remove $^{\bullet}NO_2$ and ascorbate reaction derivatives (i.e., chemically modified GDP−NO_2 adduct) as well as unreacted ascorbate from oxidized Rho GTPases. RhoA protein derived from this treatment is referred to herein as "NO_2-treated RhoA". Treatment of Rho GTPases with $^{\bullet}NO_2$ in the absence of O_2 did not produce Rho-SNO (not shown). Thus, under our experimental conditions (anaerobic conditions), Rho-SNO does not appear to be generated. Furthermore, even if Rho-SNO was formed (by potential O_2 contamination), treatment with ascorbate converts Rho-SNO into its sulfhydryl form. However, ascorbate treatment did not affect the stability of the $^{\bullet}NO_2$-induced RhoA disulfide (not shown). For experiments employing thiol cross-linking agents (i.e., cisplatin), RhoA was prepared using an identical procedure to that used for treatment of RhoA with $^{\bullet}NO_2$, except that various concentrations of the thiol cross-linking agent were substituted for $^{\bullet}NO_2$ and incubated for 60 min. RhoA, once treated with the thiol cross-linking agent, was not affected by ascorbate treatment (not shown). Furthermore, upon treatment with $^{\bullet}NO_2$ and thiol cross-linking agents, RhoA proteins were stable under open atmosphere and could be exposed to air. Thus, quantification, mass spectrometry, and kinetic analyses of the oxidized RhoA proteins were performed under aerobic conditions. Quantification of oxidized RhoA formed upon treatment with $^{\bullet}NO_2$ was determined using 4,4′-dithiodipyridine (*36*) according to eq 1:

$$\text{oxidized RhoA protein} = \text{untreated reactive protein sulfhydryls} - {}^{\bullet}NO_2\text{-treated protein sulfhydryls} \quad (1)$$

The amount of oxidized RhoA formed upon treatment with a thiol cross-linker was also determined using 4,4′-dithiodipyridine (*36*) and eq 1.

MALDI-TOF Mass Spectrometric Analysis. For mass spectrometric data a representative RhoAF25N protein sample was utilized because of its enhanced protein expression and functional equivalence to wt RhoA. The protein was digested with Promega sequencing grade modified Trypsin in a 25 mM ammonium bicarbonate solution (1 trypsin:10 protein by mass ratio) for 4 h at 37 °C. After the

[1] Abbreviations: Vav2 DPC, catalytic fragment from the Vav2 guanine nucleotide exchange factor that contains the DH, PH, and CRD domains (DPC); DPTA, diethylenetriaminepentaacetate; DTT, dithiothreitol; GSH, glutathione; PAO, phenylarsine oxide; mant-GDP, 2′-(or-3′)-*O*-(*N*-methylanthraniloyl)guanosine 5′-ribose diphosphate; Rac1-$Cys^{18\bullet}$ intermediate, Rac1 Cys^{18}-thiyl radical intermediate; RhoA $Cys^{16\bullet}$ intermediate, RhoA Cys^{16}-thiyl radical intermediate; RhoA $Cys^{20\bullet}$ intermediate, RhoA Cys^{20}-thiyl radical intermediate; MALDI-TOF, matrix assisted laser desorption/ionization time of flight mass spectrometry; NO, nitric oxide; $^{\bullet}NO_2$, nitrogen dioxide; RhoA-SNO, S-nitrosylated RhoA; RNS, reactive nitrogen species; ROS, reactive oxygen species; CysSH, free cysteine; $O_2^{\bullet-}$, superoxide anion radical; wt, wild type.

digestion was complete, the sample was lyophilized and then resuspended in 50% acetonitrile:0.1% trifluoroacetic acid. The sample (0.3 μL) was then spotted on an ABI (Applied Biosystems) MALDI target and then mixed with a saturated matrix solution (0.3 μL). The matrix (α-cyano-4-hydroxycinnamic acid; Sigma) was previously recrystallized and then resuspended in 50% acetonitrile:0.1% trifluoroacetic acid: 20 mM ammonium citrate. MALDI mass spectrometer analyses were performed on an ABI 4700 Voyager TOF/TOF with pulsed ion extraction, and the data were analyzed using "Data Explorer-Software (ABI)".

Kinetic Measurements of Rho GTPase Guanine Nucleotide Exchange. The buffer used for the fluorescence measurements contained 20 mM mant-GDP and 100 μM DPTA in assay buffer (5 mM ammonium acetate, 5 mM $MgCl_2$, and 50 mM NaCl, pH 7.5). Rho GTPase guanine nucleotide exchange was initiated by addition of untreated, $^{\bullet}NO_2$- or cisplatin (20 μM)-treated Rho GTPase into the assay buffer containing mant-GDP (20 mM), and the exchange of RhoA-bound GDP with mant-GDP was measured as a change in the fluorescence intensity over time using a LS50B Perkin-Elmer fluorimeter (*34*, *37*). To aid in detecting the intrinsic rate of RhoA guanine nucleotide exchange under our experimental conditions, excess RhoA protein (10 μM) was employed.

Kinetic Measurements of Vav2 DPC-Mediated Rho GTPase Guanine Nucleotide Exchange. Vav2 DPC-mediated Rho GTPase guanine nucleotide exchange was initiated by addition of Vav2 DPC (1 μM) into assay buffer containing mant-GDP (20 mM) as well as untreated, $^{\bullet}NO_2$-, or cisplatin-treated Rho GTPase (10 μM) for 30 min, and the exchange of mant-GDP to Rho GTPase was measured as a change in the fluorescence intensity over time using a LS50B Perkin-Elmer fluorimeter as previously described (*34*). Although this fragment of Vav2 containing the DH, PH, and CRD domains (DPC) can facilitate RhoA guanine nucleotide exchange, we have previously shown that the DPC fragment is more active on Rac1 relative to RhoA *in vitro* (*34*). Hence, higher concentrations of Vav2 DPC (1 μM) were employed for RhoA measurements. Typically, the catalytic rate of enzymatic processes can be determined by using the enzyme concentrations less than its dissociation constant (K_D) (*38*). Thus, the enhanced rate of the Vav2 DPC-mediated RhoA guanine nucleotide exchange presented in this study does not correspond to the true rate, as shown in our previous studies (*34*).

Coprecipitation of RhoA with a Catalytically Active Fragment of Vav2. To determine if oxidation of RhoA (RhoA S−S) interferes with binding to the catalytically active tridomain of Vav2 (termed DPC; and contains the DH, PH, and CRD domains), an immunoprecipitation pull-down assay was employed. For precipitation of the overexpressed 6 × His-tagged Vav2 DPC, Ni-NTA Magnetic Agarose Beads (Qiagen GmbH) were used. Ten microliters of a 5% Ni-NTA Magnetic Agarose Beads/Vav2 DPC protein suspension (1 mg/mL of protein) was added to oxidized RhoA, purified nucleotide-free apoRhoA, and apoRas prepared as previously described (*39*, *40*) and incubated for 2 h at 4 °C. The supernatants were separated from the beads by centrifugation, and the beads were washed three times with washing buffer containing 50 mM NaH_2PO_4 (pH 8), 300 mM NaCl, 20 mM imidazole, 0.05% Tween 20. The proteins were then eluted from the beads with 25 μL of elution buffer containing 50 mM NaH_2PO_4 (pH 8), 300 mM NaCl, 250 mM imidazole, 0.05% Tween 20. An equal volume of 2× sample buffer supplemented with β-mercaptoethanol was added to the eluates, and the samples were boiled for 5 min and centrifuged for 30 s at 12000*g* at room temperature. The supernatants were collected and separated by SDS/PAGE (15% polyacrylamide gel) and transferred onto PVDF membranes. Samples were subjected to immunoblot analysis and visualized with the alkaline phosphatase (AP)-reaction solution. The primary antibodies used were anti-RhoA, anti-His, and anti-panRas (Santa Cruz Biotechnology) mouse monoclonal antibodies. Secondary peroxidase-conjugated anti-mouse horseradish antibodies were purchased from Amersham Biosciences.

RESULTS

The intrinsic guanine nucleotide exchange properties of wt and mutant RhoA proteins were characterized prior to addition of redox agents, platin, and arsenic compounds. Although the biochemical and redox properties of wt and F25N RhoA are nearly identical (not shown), wt RhoA was also used to confirm results obtained from F25N RhoA. The RhoA variants, C16A and C20A were generated in the context of the F25N mutation, as the RhoA F25N mutant expresses at higher yields in *Escherichia coli* (*41*).

$^{\bullet}NO_2$-Mediated Oxidation of Rho GTPases. RhoA GTPases treated with $^{\bullet}NO_2$ were characterized for oxidation using 4,4′-dithiodipyridine (*36*) according to eq 1. Results shown in Figure 1A indicate that $^{\bullet}NO_2$ promotes oxidation of F25N and wt RhoA, but not wt Rac1. The samples were further analyzed by MALDI-TOF mass spectrometry, demonstrating that the observed oxidation is due to formation of a disulfide between Cys^{16} and Cys^{20} (Cys^{16}-Cys^{20}) in both F25N (Figure 2) and wt RhoA (not shown). Consistent with this observation, the RhoA variants, C16A/F25N and C20A/F25N, that lack a cysteine at these positions, do not form a protein disulfide upon the treatment of $^{\bullet}NO_2$ (Figure 2). Moreover, wt Rac1 and wt Cdc42 possess a redox-active cysteine (Cys^{18} in Rac1 numbering, equivalent to RhoA Cys^{20}), but lack the cysteine residue equivalent to RhoA Cys^{16} (*8*), and thus do not form a disulfide (not shown).

Although ∼2 μM $^{\bullet}NO_2$ can promote wt RhoA guanine nucleotide dissociation (*8*), RhoA disulfide (Cys^{16}-Cys^{20}) formation was observed at $^{\bullet}NO_2$ concentrations between 3 and 5 μM (Figure 1 and 2). These results suggest that RhoA Cys^{16}-Cys^{20} disulfide formation occurs after guanine nucleotide dissociation, consistent with observations that the cysteines in GDP-bound RhoA do not possess the right distance and geometry to form a disulfide (*9*).

Results shown in Figure 1B indicate that cisplatin can oxidize both wt and F25N RhoA. However, the mode of oxidation for cisplatin-treated RhoA is likely to differ from $^{\bullet}NO_2$-mediated RhoA disulfide formation, as cisplatin oxidizes adjacent protein sulfhydryls by formation of a thiol−cisplatin−thiol adduct (*23*, *24*). Given that PAO has been shown to inactivate RhoA by bridging the Cys^{20} and Cys^{16} thiols (*29*), we postulated that cisplatin oxidizes F25N and wt RhoA (Figure 1B) by a similar mechanism, i.e., by formation of a complex with the Cys^{20} and Cys^{16} thiols contained within the RhoA GXXXCGK(S/T)C motif. We

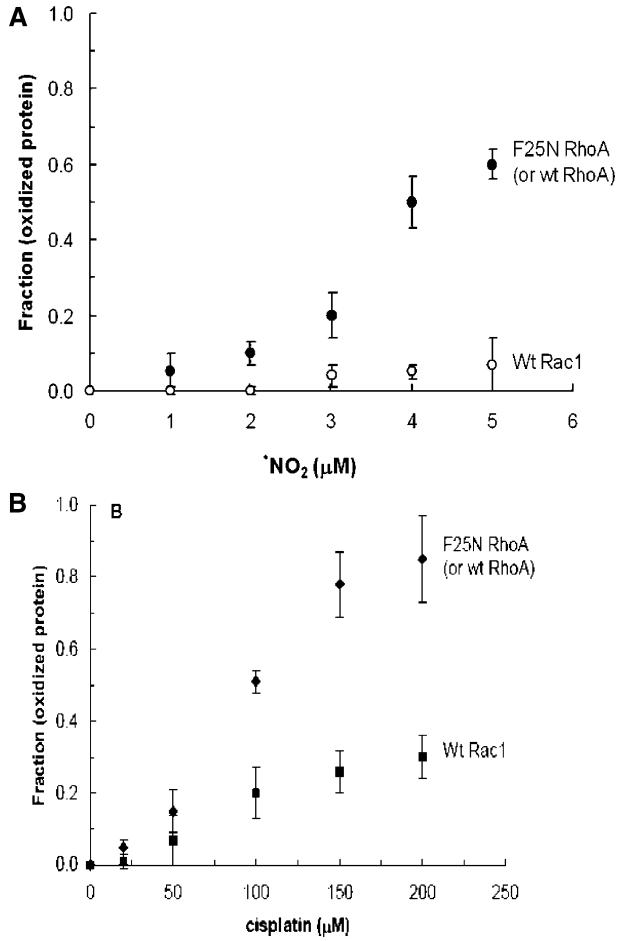

FIGURE 1: A. Redox-mediated oxidation of Rho GTPases. Treatment of F25N RhoA (or wt RhoA) (1 μM) with $^{\bullet}NO_2$ induces a concentration dependent increase in protein fraction oxidation (●). Treatment of wt Rac1 (1 μM) with $^{\bullet}NO_2$ does not induce protein oxidation (○). Details of $^{\bullet}NO_2$- mediated oxidation and detection of Rho GTPases are described in Materials and Methods. The data presented in the figure are mean values of triplicate measurements. B. Cisplatin-mediated oxidation of Rho GTPases. Treatment of F25N RhoA (or wt RhoA) (1 μM) with cisplatin induces a concentration dependent increase in protein fraction oxidation (◆). Treatment of wt Rac1 (1 μM) with cisplatin induces a concentration dependent increase in protein oxidation to a lesser extent (■). The data presented in the figure are mean values of triplicate measurements.

have also observed that cisplatin can oxidize wt Rac1 (Figure 1B), albeit to a lesser degree relative to wt and F25N RhoA. As thiol cross-linkers can react with a single sulfhydryl to produce a thiol−cisplatin adduct as well as bridge two adjacent thiols of appropriate distance and geometry to produce a thiol−cisplatin−thiol adduct, we speculate that treatment of cisplatin with wt Rac1 produces an oxidized form of wt Rac1, a Rac1 Cys^{18} thiol−cisplatin adduct.

Unlike $^{\bullet}NO_2$, however, cisplatin-mediated oxidation of F25N and wt RhoA requires excess cisplatin (Figure 1B). For example, 50% oxidation of F25N and wt RhoA can be obtained at an $^{\bullet}NO_2$ concentration of ~4 μM, while ~11 μM arsenate or ~100 μM cisplatin is required to obtain an equivalent amount (50%) of oxidized RhoA. Among the tested thiol cross-linkers (Table 1), the most effective agent for RhoA oxidation is arsenate, while the least effective is oxaliplatin, with the order of effectiveness in oxidation as follows: arsenate > arsenic trioxide > cisplatin > oxaliplatin.

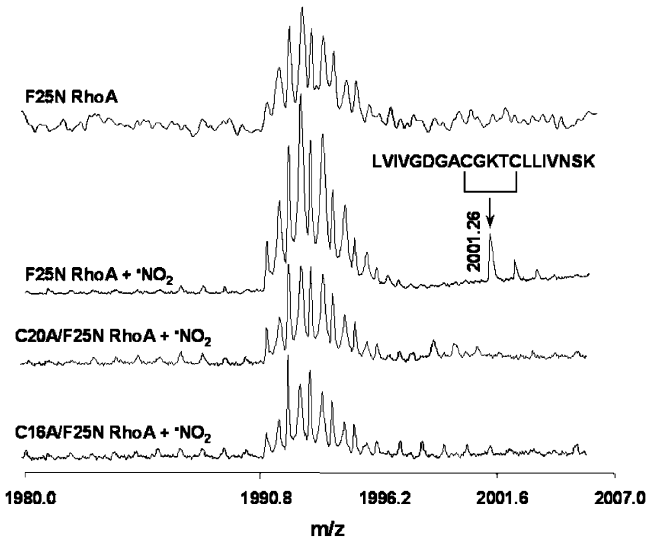

FIGURE 2: Mass spectrometric analysis of oxidized $^{\bullet}NO_2$-mediated RhoA. Wt and variant RhoA proteins (1 μM) were treated with $^{\bullet}NO_2$ (~5 μM) followed by addition of ascorbate (1 mM). Methods for detection of RhoA protein disulfides using MALDI-TOF are described in Materials and Methods. A mass peak ($[LVIVGDGACGKTCLLIVNSK + H]^+ = 2001.26$ Da) representing a peptide containing disulfide between Cys^{16} and Cys^{20} upon the treatment of $^{\bullet}NO_2$ was found in F25N RhoA, but not the C16A/F25N and C20A/F25N RhoA variants. A peptide fragment mass peak ($[LVIVGDGACGKTCLLIVFSK + H]^+ = 2036.1$ Da) containing disulfide between Cys^{16} and Cys^{20} was also detected (not shown) upon treatment of wt RhoA with $^{\bullet}NO_2$. Multiple mass peaks are observed for the RhoA F25N sample in the range from 1990 to 1996 Da. As these peaks overlap with the mass peaks obtained for the RhoA F25N variants, they most likely represent fragments that are not modified upon trypsin digestion of the Rho protein samples treated with $^{\bullet}NO_2$. Furthermore, as the peaks detected in the 1990−1996 Da mass range do not correspond to trypsin-digested Rho protein fragments that possess RhoA Cys^{16} and Cys^{20}, they were not assigned.

Table 1: Dose-Dependent Oxidation of F25N RhoA by Various Thiol Cross-Linking Agents

	50% oxidation	80% oxidation
$^{\bullet}NO_2$	~4 ± 1	~5 ± 2
arsenate (AsO_4^{3-})	11 ± 6	15 ± 7
arsenic trioxide (As_2O_3)	87 ± 9	156 ± 8
cisplatin	102 ± 4	197 ± 5
oxaliplatin	189 ± 8	286 ± 11

Kinetics of Oxidized RhoA Treated with $^{\bullet}NO_2$. Results shown in Figure 3 indicate that the guanine nucleotide exchange rate observed for $^{\bullet}NO_2$-treated F25N RhoA (10 μM) is largely inhibited compared to that of untreated F25N RhoA. However, reduction of the Cys^{16}-Cys^{20} disulfide by GSH restores the rate of guanine nucleotide exchange for F25N RhoA (Figure 3). GSH does not affect the intrinsic rate of GDP exchange for untreated F25N RhoA (not shown). Similar to F25N RhoA, $^{\bullet}NO_2$ inhibits the rate of GDP exchange for wt RhoA, which is restored by GSH (not shown), indicating that the redox properties of wt RhoA are similar to those of F25N RhoA. In contrast, minimal perturbation in the rate of GDP exchange is observed for both $^{\bullet}NO_2$-treated C16A/F25N and C20A/F25N RhoA (Figure 3). These kinetic results suggest that $^{\bullet}NO_2$-mediated

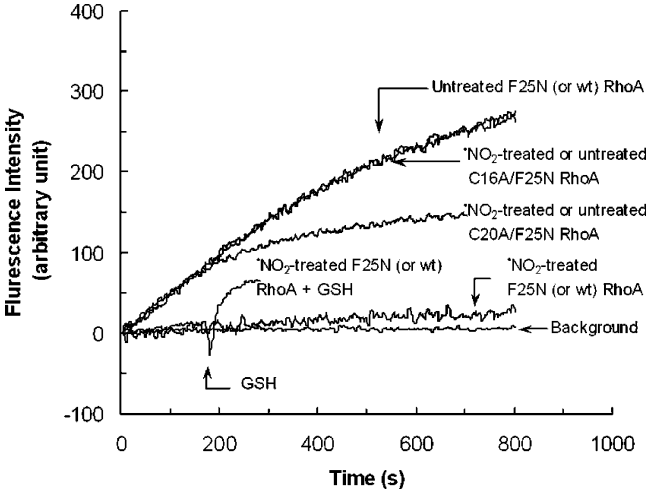

FIGURE 3: Kinetic measurements of RhoA GTPase guanine nucleotide exchange. The apparent intrinsic guanine nucleotide dissociation rates of untreated, $^{\bullet}NO_2$-treated variant RhoA GTPases (10 μM) were measured using fluorescence mant-GDP as described in Materials and Methods. The changes in fluorescence intensity were fit to a simple exponential association to give rates of untreated and $^{\bullet}NO_2$-treated F25N RhoA of 0.0019 and <0.0001 s^{-1}, respectively. The rates of untreated and $^{\bullet}NO_2$-treated C16A/F25N RhoA were determined to be 0.0017 and 0.0016 s^{-1}, respectively and are indistinguishable. The rates of untreated and $^{\bullet}NO_2$-treated C20A/F25N RhoA, determined to be 0.0034 and 0.0035 s^{-1}, respectively, are also nearly identical. Given that the rates of both untreated and $^{\bullet}NO_2$-treated C20A/F25N RhoA are nearly identical, the graphic representation for $^{\bullet}NO_2$-treated C20A/F25N RhoA was omitted. The guanine nucleotide exchange rate of $^{\bullet}NO_2$-treated RhoA in the presence of GSH (1 mM), as indicated by arrow, was determined to be 0.0031 s^{-1}. The regression values associated with all fits were $r^2 > 0.9985$.

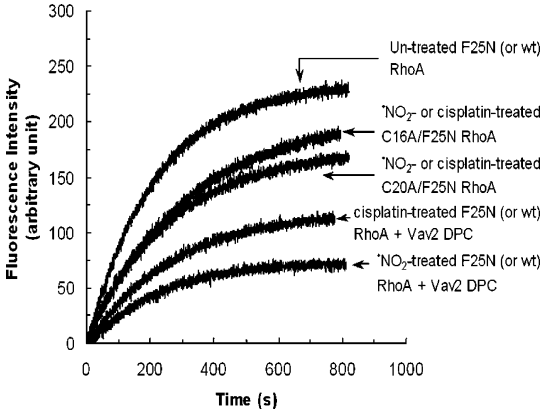

FIGURE 4: Kinetic measurements of Vav2 DPC-mediated RhoA GTPase guanine nucleotide exchange. The effect of Vav2 DPC (1 μM) on the rate of guanine nucleotide exchange for $^{\bullet}NO_2$ ($\sim$4 μM)- and cisplatin (100 μM)-treated RhoA (10 μM) was examined, as described in Materials and Methods. The changes in fluorescence intensity were fit to a simple exponential association to give Vav2 DPC-enhanced rates for untreated F25N (or wt), cisplatin-treated F25N (or wt), and $^{\bullet}NO_2$-treated F25N (or wt) RhoA GTPase corresponding to 0.0094, 0.0018, and 0.0008 s^{-1}, respectively. The rates of $^{\bullet}NO_2$-treated C16A/F25N and cisplatin-treated C16A/F25N, $^{\bullet}NO_2$-treated C20A/F25N and cisplatin-treated C20A/F25N RhoA GTPase (not present) were 0.0057, 0.0059, 0.0054, and 0.0058 s^{-1}, respectively. These rates were not enhanced by addition of the catalytically active Vav2 DPC fragment. For all fits, the regression values were $r^2 > 0.9995$.

Cys^{16}-Cys^{20} disulfide formation prevents F25N and wt RhoA guanine nucleotide exchange.

As shown in Figure 3, the rate of GDP exchange for untreated and $^{\bullet}NO_2$-treated C20A/F25N RhoA is $\sim$2-fold faster than that of F25N and C16A/F25N RhoA. Moreover, GDP exchange for untreated and $^{\bullet}NO_2$-treated C20A/F25N RhoA is saturated at earlier times compared with that of F25N and C16A/F25N RhoA (Figure 3). Although it is unclear why incomplete GDP exchange (saturation at an earlier stage) occurs in untreated and $^{\bullet}NO_2$-treated C20A/F25N RhoA, we postulate that the 2-fold enhanced rate of GDP exchange results from destabilization of RhoA nucleotide interactions. In the Rho GTPase Cdc42, the Phe^{28} side chain forms packing interactions with the guanine nucleotide base that contributes to Cdc42 guanine nucleotide binding (*11*, *42*). The structural topology of RhoA (*9*) is similar to that of Cdc42 (*11*). As Phe^{30} in RhoA (equivalent to Cdc42 Phe^{28}) is proximal to the redox-active Cys^{20} ($\sim$3.6 Å) (*9*), it is possible that mutation of RhoA Cys^{20} into alanine may alter interactions between RhoA Phe^{30} with bound GDP or possibly other proximal residues that interact with GDP (i.e., α-phosphate of bound GDP, Pro^{31} (equivalent to Ha-Ras Val^{29}) that interacts with RhoA-bound GDP ribose), resulting in an enhanced rate of GDP exchange. In fact, mutation of Phe^{28} to a leucine in Cdc42 greatly enhances the rate of guanine nucleotide dissociation (*42*).

Kinetics of $^{\bullet}NO_2$ and Cisplatin-Mediated Oxidized RhoA in the Presence and Absence of the Vav2 Rho GEF Catalytic Fragment, DPC. To explore the effect of Rho GEFs on $^{\bullet}NO_2$- and cisplatin-treated RhoA guanine nucleotide dissociation, a Rho GTPase-specific GEF fragment, which contains an active catalytic tridomain (DPC) of Vav2 (*34*), was added to the assay. RhoA GTPases (10 μM) were used (Figure 4) in GEF-mediated guanine nucleotide exchange assays to allow comparison with the intrinsic rate of RhoA guanine nucleotide exchange (Figure 3). Figure 4 shows that Vav2 DPC is able to enhance F25N and wt RhoA guanine nucleotide exchange, consistent with our previous studies (*34*). However, little stimulation of guanine nucleotide exchange is observed in the presence of Vav2 DPC for wt RhoA samples treated with $^{\bullet}NO_2$ or cisplatin (Figure 4). Furthermore, given that cisplatin is highly reactive with thiols (*23*, *24*) and the rate of guanine nucleotide exchange for both $^{\bullet}NO_2$- or cisplatin-treated C16A/F25N and C20A/F25N RhoA is enhanced by the Vav2 DPC fragment (Figure 4), oxidative formation of either the RhoA Cys^{20}-Cys^{16} disulfide or RhoA Cys^{20}-cisplatin-Cys^{20} bridge may block Vav2 DPC-mediated RhoA guanine nucleotide exchange under our experimental conditions.

Similar to cisplatin, pretreatment of RhoA with other potential thiol bridging agents, such as oxaliplatin (between 50 and 200 μM), arsenate (between 1 and 20 μM), and arsenic trioxide (between 10 and 100 μM), shows a concentration-dependent inhibition of guanine nucleotide exchange (not shown), which is consistent with dose-dependent thiol cross-linker-mediated oxidation of RhoA (Table 1).

Electrospray ionization mass spectrometry analyses indicate that RhoA samples containing either a Cys^{16}-Cys^{20} disulfide or Cys^{16}-cisplatin-Cys^{20} bridge lack guanine nucleotide (not shown), suggesting that $^{\bullet}NO_2$- and cisplatin-mediated formation of RhoA Cys^{16}-Cys^{20} and RhoA Cys^{16}-cisplatin-Cys^{20} promotes release to GDP to generate a nucleotide-deficient form of RhoA.

Coprecipitation of Oxidized RhoA and Vav2 DPC. Last we sought to determine if the RhoA samples containing a

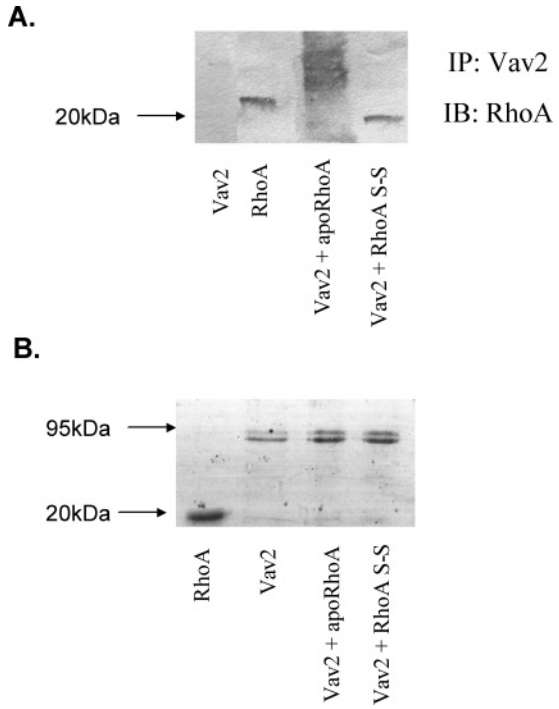

FIGURE 5: Coprecipitation of oxidized RhoA and Vav2 DPC. A. Anti-RhoA blot of purified Vav2 DPC co-immunoprecipitated with apoRhoA and oxidized RhoA (RhoA S−S) from Ni-NTA magnetic agarose beads. Assays were performed using the pull-down assay as described in the Materials and Methods section with the appropriate RhoA antisera. B. Samples from panel A were subjected to Coomassie Blue staining as a standard control. All data are representative of three independent experiments.

Cys^{16}-Cys^{20} disulfide bridge interfered with its interaction with Vav2 DPC which would support our findings that RhoA oxidation may block Vav2 DPC-mediated RhoA guanine nucleotide exchange. Prior to coprecipitation, MALDI-mass spectrometry was preformed to verify that the Cys^{16}-Cys^{20} disulfide bridge remained intact over time. The analysis demonstrated an identical spectrum as oxidized wt RhoA, indicating that the RhoA disulfide cross-link remained stable. Therefore, examination of coprecipitation was continued by immobilizing Vav2 DPC on nickel beads and incubating with oxidized RhoA. Figure 5 demonstrates that oxidized RhoA (RhoA S−S) can be detected at the same molecular weight as free (unbound) RhoA but was not found to coprecipitate with Vav2 DPC. In contrast, apoRhoA did coprecipitate with Vav2 DPC as indicated by anti-RhoA immunoblot detection at a higher molecular weight than free RhoA. To demonstrate specificity of the Vav2 DPC interaction with RhoA, the analysis was also conducted with apoRas which does not bind to the Vav2 DPC. As expected, data illustrated in Figure 5 indicates that Ras is unable to bind to Vav2 DPC (not shown). Therefore, we can conclude that the Cys^{16}-Cys^{20} disulfide bridge caused by oxidation of RhoA interferes with RhoA specific interactions with the Rho GEF catalytic fragment, Vav2 DPC, thereby preventing Vav2 DPC-mediated guanine nucleotide exchange of oxidized RhoA.

DISCUSSION

Recent studies in pulmonary artery endothelial cells suggest that RhoA and Rac1 show opposing responses to hypoxia and reoxygenation resulting in altered phosphatidylinositol-3 kinase (PI3K) activity and modulation of endothelial permeability (*12*). It has been also shown that Rac1-mediated ROS production results in the downregulation of RhoA activity in HeLa cell lines (*43*), where the interaction of Rac1 with the $O_2^{\bullet-}$-producing NADPH oxidase complex mediates activation of NADPH oxidase (*44*). Thus, under certain conditions, RhoA and Rac1 may respond antagonistically to cellular redox signals. Moreover, inhibition of RhoA has been shown to increase production of NO by endothelial nitric oxide synthase (*45*−*49*). In these studies, RhoA inhibition was achieved by a variety of approaches, including use of dominant negative RhoA variants, statins, bacterial toxins, and the Rho-binding domain of Rho kinase (ROCK). RhoA also regulates NO production *via* the PI3K/protein kinase Akt pathway (*50*). Inhibition of RhoA or Rho kinase can lead to the rapid phosphorylation and activation of Akt *via* PI3K, resulting in increase in NO production from endothelial nitric oxide synthase (*51*). Inhibition of the RhoA/Rho kinase pathway in endothelial cells may also stimulate Akt activity by decreasing the activity of the PTEN (phosphatase and tensin homologue deleted on chromosome Ten) (*52*). However, it is unclear whether the alterations observed in Rho GTPase-mediated signaling and NO production observed in theses studies result from direct redox regulation of Rho GTPases and/or whether modulation of Rho GTPases function occurs indirectly.

Distinct Redox Regulation of RhoA. We have previously demonstrated that reaction of redox agents, ROS and RNS, with RhoA, Cdc42, and Rac1 stimulates guanine nucleotide release (*8*). In contrast to Rac1 and Cdc42, RhoA contains an extra cysteine (Cys^{20}, RhoA numbering) in the redox-active motif. Results from the present study indicate that the presence of this cysteine promotes formation of an intramolecular disulfide that prevents guanine nucleotide binding and GEF association, thereby causing RhoA inactivation. Thus, redox agents may function to downregulate RhoA activity under conditions that stimulate Rac1 and Cdc42 activity. The opposing functions of these GTPases (i.e., RhoA versus Rac1) may be due in part to their direct differential response to redox agents.

Potential Mechanism of RhoA Disulfide Formation. According to the RhoA−GDP crystal structure (*9*), the buried RhoA Cys^{16} thiol is ∼10.3 Å away from the solvent accessible redox-active RhoA Cys^{20} thiol, and the α-phosphate of the bound GDP intercalates between these two RhoA cysteine thiols. Therefore, RhoA Cys^{16} and Cys^{20} thiols in the RhoA−GDP complex are not well positioned for disulfide formation. Thus, given our kinetic and mass spectrometry results, we speculate that RhoA Cys^{16}-Cys^{20} disulfide formation may require release of the RhoA-bound guanine nucleotide to alter RhoA guanine nucleotide-binding pocket to facilitate interaction between the RhoA Cys^{16} and Cys^{20} thiols.

Based on these structural considerations in conjunction with our previous studies (*8*, *53*, *54*), we propose that $^{\bullet}NO_2$-mediated disulfide formation involves two successive redox cycles. In the first cycle, two $^{\bullet}NO_2$ are consumed to produce GDP-deficient RhoA and a free GDP−NO_2 adduct. In this first cycle, reaction of the RhoA Cys^{20} thiol with $^{\bullet}NO_2$ produces a RhoA-thiyl radical, postulated to be GDP-bound RhoA $Cys^{20\bullet}$. The Cys^{20}-thiyl radical of GDP-bound RhoA withdraws an electron from the bound GDP guanine base to produce a RhoA-bound G$^{\bullet}$−DP intermediate. Another $^{\bullet}NO_2$

can then be consumed to produce a GDP-deficient RhoA and a GDP−NO_2 adduct. GDP-deficient RhoA can then bind fresh GDP to produce GDP-bound RhoA, or can undergo a second redox cycle. In the second cycle, additional $^{\bullet}NO_2$ can be consumed to produce a stable GDP-deficient oxidized RhoA (GDP-deficient RhoA Cys^{16}-Cys^{20}). We speculate that when the GDP−NO_2 adduct is released from RhoA, the RhoA Cys^{16} thiol may become accessible to $^{\bullet}NO_2$. If so, a third $^{\bullet}NO_2$ can react with either the Cys^{16} or Cys^{20} thiol of GDP-deficient RhoA to produce either GDP-deficient RhoA $Cys^{16\bullet}$ or GDP-deficient RhoA $Cys^{20\bullet}$ intermediate. In either case, a radical reaction between a thiyl radical and thiol could produce a GDP-deficient RhoA disulfide anionic radical (GDP-deficient RhoA Cys^{16}-$Cys^{20\bullet-}$), which can be quenched by ascorbate to produce a GDP-deficient RhoA Cys^{16}-Cys^{20}. It is also possible that additional $^{\bullet}NO_2$ (third and fourth $^{\bullet}NO_2$, including the amount of consumed $^{\bullet}NO_2$ from the first redox cycle) may be consumed to produce GDP-deficient RhoA Cys^{16}-Cys^{20}, where the third and fourth $^{\bullet}NO_2$ react with both the Cys^{16} and Cys^{20} thiols of GDP-deficient RhoA to produce a biradical GDP-deficient RhoA on the Cys^{16} and Cys^{20} thiols, i.e., GDP-deficient RhoA $Cys^{16\bullet}$-$Cys^{20\bullet}$. An intraradical reaction between $Cys^{16\bullet}$ and $Cys^{20\bullet}$ of the GDP-deficient RhoA could also produce a GDP-deficient RhoA Cys^{16}-Cys^{20} disulfide. Given that $^{\bullet}NO_2$ may also react with other potential redox-active residue(s) in RhoA, titration of RhoA with various quantified amounts $^{\bullet}NO_2$ may not provide the exact redox stoichiometry of $^{\bullet}NO_2$ used in the formation of the GDP-deficient RhoA Cys^{16}-Cys^{20} disulfide. Although we do not know the exact stoichiometry of $^{\bullet}NO_2$ consumed in formation of the disulfide, the $^{\bullet}NO_2$-mediated oxidation profile of RhoA (Figure 1) indicates that 4 equiv of $^{\bullet}NO_2$ to RhoA is required to produce nearly 60% GDP-deficient RhoA Cys^{16}-Cys^{20} disulfide, consistent with our premise that generation of GDP-deficient RhoA $Cys^{16\bullet}$-$Cys^{20\bullet}$ may be required for formation of the GDP-deficient RhoA Cys^{16}-Cys^{20} disulfide. Like $^{\bullet}NO_2$, $O_2^{\bullet-}$ may also mediate the RhoA redox cycling, since $O_2^{\bullet-}$ can also react with RhoA Cys^{20} thiol to produce RhoA $Cys^{20\bullet}$ (*8*). If so, formation of the GDP-deficient RhoA $Cys^{20\bullet}$ and/or $Cys^{16\bullet}$ intermediate appears to be kinetically competent, as the rate constants for reaction of $^{\bullet}NO_2$ with GSH and free cysteine ($\sim 2 \times 10^7$ and 5×10^7 M^{-1} s^{-1}, respectively) (*55*) are faster than the intrinsic rate of Ras guanine nucleotide association ($\sim 2 \times 10^6$ M^{-1} s^{-1}) (*56*). Moreover, our recent kinetic analyses indicate that the intrinsic rate of RhoA guanine nucleotide exchange (Figure 3) is similar to that of Ras (*53*). The reaction rate of the GDP-deficient RhoA Cys^{20} and/or Cys^{16} with $^{\bullet}NO_2$ may not be significantly different from that of $^{\bullet}NO_2$ with GSH and free cysteine unless the GDP-deficient RhoA Cys^{16} and/or Cys^{20} thiol becomes less accessible in GDP-deficient RhoA. Hence, the formed GDP-deficient RhoA Cys^{16} and/or Cys^{20} thiol may react with $^{\bullet}NO_2$ to produce a $^{\bullet}NO_2$-induced GDP-deficient RhoA $Cys^{20\bullet}$ and/or $Cys^{16\bullet}$ intermediate, which does not associate with GDP readily as the rate of GDP exchange is reduced for this state of RhoA.

Our postulated redox cycle indicates that initially addition of $^{\bullet}NO_2$ to RhoA facilitates RhoA GDP dissociation (the first redox cycle). However, when $^{\bullet}NO_2$ is in excess (i.e., 3−4 equiv $^{\bullet}NO_2$ to RhoA), RhoA is inactivated by formation of the GDP-deficient RhoA Cys^{16}-Cys^{20} disulfide (the second redox cycle). However, the GXXXXGK(S/T)C motif-containing GTPases (i.e., Rac1), that lacks a second cysteine near the guanine nucleotide binding site, can only undergo the first redox cycle as Rac1 does not have a second cysteine necessary for disulfide formation.

Our data also indicates that the GDP-deficient Cys^{16}-Cys^{20} disulfide form of RhoA cannot associate with the Rho GEF catalytic tridomain (DPC) of Vav2 to promote GEF-mediated guanine nucleotide exchange. This is perhaps not too surprising, given the available structural and biochemical information available on Rho−GEF interactions (*57*). DH domains of Rho family GEFs cause remodeling of the switch regions to promote disorganization of the nucleotide binding pocket and direct occlusion of the Mg^{2+} binding site, resulting in enhanced guanine nucleotide exchange. Although the phosphate binding loop undergoes minimal structural perturbation upon interaction of the GTPase with the GEF DH domain, the primary alteration of this loop involves Cys^{18} in Rac1 (Cys^{20} in RhoA) which moves out of bond forming distance with the α-phosphate and facilitates guanine nucleotide exchange. Thus, our data indicates that RhoA S−S represents an inactive form of RhoA, which cannot bind guanine nucleotide substrates nor interact with exchange factors.

RhoA Regulation by Various Anticancer Drugs. Results from these studies also indicate that the nucleic acid-targeting anticancer drugs, platins (i.e., cisplatin and oxaliplatin) and arsenic compounds can inactivate RhoA. These results are not unexpected, given recent studies that the thiol cross-linker, PAO, inactivates RhoA by forming a bridge between Cys^{20} and Cys^{16} in RhoA (*29*). Thus, in addition to PAO, other thiol cross-linkers (i.e., platins as well as arsenate and arsenic trioxide) may inactivate RhoA by bridging Cys^{20} and Cys^{16}. Thus, it is feasible that a number of thiol cross-linkers including platinated-chemotherapeutic agents may form complexes with GXXXCGK(S/T)C motif-containing GTPases (i.e., RhoA and RhoB) causing their inactivation. Although platins are known for their ability to target nucleic acids and are currently used as anticancer agents (*13*−*16*), one or many of the platin-induced cytotoxic effects may be due to oxidation of GXXXCGK(S/T)C motif-containing GTPases (i.e., RhoA). It is also possible that select platin and arsenic agents may be useful in treatment of human disease states (i.e., cancer) caused by the aberrant upregulation of GXXXCGK(S/T)C motif-containing GTPases.

Potential Mechanism of RhoA−*Cisplatin Adduct Formation.* Given that cisplatin reacts with thiols (*23*, *24*), we speculated that cisplatin may be able to cross-link with Cys^{20} and Cys^{16} of RhoA to produce a RhoA−cisplatin adduct (i.e., RhoA thiol−cisplatin−thiol). As the RhoA Cys^{20} but not the Cys^{16} site is solvent accessible (*9*), cisplatin may initially react with the RhoA Cys^{20} thiol. However, cisplatin may not be able to immediately bridge between the Cys^{20} and Cys^{16} thiols, since the GDP-α phosphate in the GDP-bound form of RhoA may prevent further reaction with the Cys^{16} thiol. Moreover, the distance between the Cys^{20} and Cys^{16} thiols in the GDP-bound form of RhoA is ~10.3 Å, which is likely to prevent direct cross-linking (*9*). Therefore, formation of a RhoA thiol−cisplatin−thiol adduct may require a conformational rearrangement in RhoA. Given the proximity of Cys^{20} to residues in Ras (such as Phe^{30} etc.) that form interactions with the bound GDP (*9*), reaction of cisplatin

with the Cys^{20} thiol may destabilize guanine nucleotide binding interactions leading to release of RhoA-bound GDP to produce GDP-deficient RhoA. It has previously been shown that the GDP-deficient form of Ras retains similar secondary structure, but possesses a molten-like tertiary structure (*58*). Although these studies were not conducted on RhoA, it is likely that the guanine nucleotide-binding site of GDP-deficient RhoA is more conformationally dynamic and solvent accessible relative to GDP-bound RhoA. Thus, if reaction of cisplatin with the Cys^{20} thiol promotes release of GDP from RhoA, the Cys^{20} and Cys^{16} thiol side chains in GDP-deficient RhoA may possess enough conformational mobility to bridge with cisplatin.

On the basis of these structural considerations, we propose a two-step RhoA thiol−cisplatin−thiol formation mechanism. Cisplatin reacts initially with the RhoA Cys^{20} thiol to produce GDP-deficient RhoA. Once GDP dissociates from RhoA, the Cys^{16} thiol of RhoA is likely to be more solvent exposed and conformationally mobile, thus facilitating reaction with the RhoA Cys^{20}−cisplatin adduct to bridge the Cys^{20} and Cys^{16} thiols, thereby inhibiting RhoA GDP exchange.

This mechanism explains how PAO bridges the RhoA Cys^{20} and Cys^{16} thiols, and possibly other thiol cross-linking agents, i.e., arsenate and arsenic trioxide, which can bridge two vicinal thiols (*26*−*29*). Intriguingly, As_2O_3 has gained therapeutic importance because it has been shown to be very effective clinically in the treatment of acute leukemia (*28*). Arsenate has been also shown to inactivate a plant redox-active enzyme, carboxy arabinitol 1-phosphate phosphatase, by bridging vicinal thiols (*27*).

In summary, the results described herein indicate that reaction of redox agents (i.e., $^{\bullet}NO_2$) with RhoA can initially stimulate RhoA guanine nucleotide dissociation. However, RhoA is subsequently inactivated through formation of an intramolecular disulfide that prevents guanine nucleotide binding and GEF association, thereby causing RhoA inactivation. Thus, redox agents may function to downregulate RhoA activity under conditions that may stimulate Rac1 and Cdc42 activity. The opposing functions of these GTPases may be due in part to their differential redox regulation. In addition, the platinated-chemotherapeutic agents, cisplatin and oxaliplatin, which are best known for targeting nucleic acids, react with RhoA, but not Rac1 or Cdc42, to produce a RhoA thiol−cisplatin−thiol adduct, leading to inactivation of RhoA. Similarly, certain arsenic complexes (i.e., arsenate and arsenic trioxide) may inactivate RhoA by bridging the cysteine residues in the GXXXCGK(S/T)C motif. Thus, in addition to redox-mediated regulation of RhoA by various redox agents (*54*), platinated-chemotherapeutic agents and arsenic complexes may differentially modulate the activity of Rho family GTPases leading to inactivation of GTPases containing the GXXXCGK(S/T)C motif (i.e., RhoA and RhoB). While PAO and cisplatin can also react with GTPases containing a GXXXCGK(S/T)C motif and lead to inactivation of the GTPases, the reaction occurs through a distinct non-radical mediated reaction. However, critical to both reactions is the generation of a conformationally mobile nucleotide-free state of the GTPases which allows disulfide or cross-linking to occur.

ACKNOWLEDGMENT

We thank Constance A. Rogers and MinQi Lu for the preparation of protein samples used in this study. We thank Dr. Stephen Chaney (UNC-CH) for generously providing cisplatin and oxaliplatin for these studies. We also thank Dr. Debadeep Bhattacharyya and Dr. Jaap Van Buul for helpful discussions and critical feedback.

REFERENCES

1. Wennerberg, K., Rossman, K. L., and Der, C. J. (2005) The Ras superfamily at a glance, *J. Cell Sci. 118*, 843−846.
2. Jaffe, A. B., and Hall, A. (2005) Rho GTPases: biochemistry and biology, *Annu. Rev. Cell Dev. Biol. 21*, 247−269.
3. Etienne-Manneville, S., and Hall, A. (2002) Rho GTPases in cell biology, *Nature 420*, 629−635.
4. Takeya, R., and Sumimoto, H. (2003) Molecular mechanism for activation of superoxide-producing NADPH oxidases, *Mol. Cells 16*, 271−277.
5. Bokoch, G. M., and Knaus, U. G. (2003) NADPH oxidases: not just for leukocytes anymore!, *Trends Biochem. Sci. 28*, 502−508.
6. DerMardirossian, C., and Bokoch, G. M. (2005) GDIs: central regulatory molecules in Rho GTPase activation, *Trends Cell Biol. 15*, 356−363.
7. Karnoub, A. E., Symons, M., Campbell, S. L., and Der, C. J. (2004) Molecular basis for Rho GTPase signaling specificity, *Breast Cancer Res. Treat. 84*, 61−71.
8. Heo, J., and Campbell, S. L. (2005) Mechanism of redox-mediated guanine nucleotide exchange on redox-active Rho GTPases, *J. Biol. Chem. 280*, 31003−31010.
9. Ihara, K., Muraguchi, S., Kato, M., Shimizu, T., Shirakawa, M., Kuroda, S., Kaibuchi, K., and Hakoshima, T. (1998) Crystal structure of human RhoA in a dominantly active form complexed with a GTP analogue, *J. Biol. Chem. 273*, 9656−9666.
10. Hirshberg, M., Stockley, R. W., Dodson, G., and Webb, M. R. (1997) The crystal structure of human rac1, a member of the rho-family complexed with a GTP analogue, *Nat. Struct. Biol. 4*, 147−152.
11. Feltham, J. L., Dotsch, V., Raza, S., Manor, D., Cerione, R. A., Sutcliffe, M. J., Wagner, G., and Oswald, R. E. (1997) Definition of the switch surface in the solution structure of Cdc42Hs, *Biochemistry 36*, 8755−8766.
12. Wojciak-Stothard, B., Tsang, L. Y., and Haworth, S. G. (2005) Rac and Rho play opposing roles in the regulation of hypoxia/reoxygenation-induced permeability changes in pulmonary artery endothelial cells, *Am. J. Physiol. 288*, L749−760.
13. Wang, D., and Lippard, S. J. (2005) Cellular processing of platinum anticancer drugs, *Nat. Rev. Drug Discovery 4*, 307−320.
14. Decatris, M. P., Sundar, S., and O'Byrne, K. J. (2005) Platinum-based chemotherapy in metastatic breast cancer: the Leicester (U.K.) experience, *Clin. Oncol. (R. Coll. Radiol.) 17*, 249−257.
15. Jakupec, M. A., Galanski, M., and Keppler, B. K. (2003) Tumour-inhibiting platinum complexes−state of the art and future perspectives, *Rev. Physiol. Biochem. Pharmacol. 146*, 1−54.
16. Ettinger, D. S. (1998) The role of carboplatin in the treatment of small-cell lung cancer, *Oncology (Williston Park) 12*, 36−43.
17. Chaney, S. G., and Vaisman, A. (1999) Specificity of platinum-DNA adduct repair, *J. Inorg. Biochem. 77*, 71−81.
18. Rixe, O., Ortuzar, W., Alvarez, M., Parker, R., Reed, E., Paull, K., and Fojo, T. (1996) Oxaliplatin, tetraplatin, cisplatin, and carboplatin: spectrum of activity in drug-resistant cell lines and in the cell lines of the National Cancer Institute's Anticancer Drug Screen panel, *Biochem. Pharmacol. 52*, 1855−1865.
19. Leopold, W. R., Batzinger, R. P., Miller, E. C., Miller, J. A., and Earhart, R. H. (1981) Mutagenicity, tumorigenicity, and electrophilic reactivity of the stereoisomeric platinum(II) complexes of 1,2-diaminocyclohexane, *Cancer Res. 41*, 4368−4377.
20. Greene, M. H. (1992) Is cisplatin a human carcinogen?, *J. Natl. Cancer Inst. 84*, 306−312.
21. Sanderson, B. J., Ferguson, L. R., and Denny, W. A. (1996) Mutagenic and carcinogenic properties of platinum-based anticancer drugs, *Mutat. Res. 355*, 59−70.
22. Bose, R. N. (2002) Biomolecular targets for platinum antitumor drugs, *Mini-Rev. Med. Chem. 2*, 103−111.
23. Volckova, E., Dudones, L. P., and Bose, R. N. (2002) HPLC determination of binding of cisplatin to DNA in the presence of

biological thiols: implications of dominant platinum-thiol binding to its anticancer action, *Pharm. Res. 19*, 124−131.
24. Sadowitz, P. D., Hubbard, B. A., Dabrowiak, J. C., Goodisman, J., Tacka, K. A., Aktas, M. K., Cunningham, M. J., Dubowy, R. L., and Souid, A. K. (2002) Kinetics of cisplatin binding to cellular DNA and modulations by thiol-blocking agents and thiol drugs, *Drug. Metab. Dispos. 30*, 183−190.
25. Biaglow, J. E., and Miller, R. A. (2005) The thioredoxin reductase/thioredoxin system: novel redox targets for cancer therapy, *Cancer Biol. Ther. 4*, 6−13.
26. Valko, M., Morris, H., and Cronin, M. T. (2005) Metals, toxicity and oxidative stress, *Curr. Med. Chem. 12*, 1161−1208.
27. Heo, J., and Holbrook, G. (1999) Regulation of 2-carboxy-D-arabinitol 1-phosphate phosphatase: activation by glutathione and interaction with thiol reagents, *Biochem. J. 338*, 409−416.
28. Carter, D. E., Aposhian, H. V., and Gandolfi, A. J. (2003) The metabolism of inorganic arsenic oxides, gallium arsenide, and arsine: a toxicochemical review, *Toxicol. Appl. Pharmacol. 193*, 309−334.
29. Gerhard, R., John, H., Aktories, K., and Just, I. (2003) Thiol-modifying phenylarsine oxide inhibits guanine nucleotide binding of Rho but not of Rac GTPases, *Mol. Pharm. 63*, 1349−1355.
30. Heo, J., Staples, C. R., Halbleib, C. M., and Ludden, P. W. (2000) Evidence for a ligand CO that is required for catalytic activity of CO dehydrogenase from *Rhodospirillum rubrum*, *Biochemistry 39*, 7956−7963.
31. Vaisman, A., Lim, S. E., Patrick, S. M., Copeland, W. C., Hinkle, D. C., Turchi, J. J., and Chaney, S. G. (1999) Effect of DNA polymerases and high mobility group protein 1 on the carrier ligand specificity for translesion synthesis past platinum-DNA adducts, *Biochemistry 38*, 11026−11039.
32. Vaisman, A., and Chaney, S. G. (2000) The efficiency and fidelity of translesion synthesis past cisplatin and oxaliplatin GpG adducts by human DNA polymerase beta, *J. Biol. Chem. 275*, 13017−13025.
33. Vaisman, A., Masutani, C., Hanaoka, F., and Chaney, S. G. (2000) Efficient translesion replication past oxaliplatin and cisplatin GpG adducts by human DNA polymerase eta, *Biochemistry 39*, 4575−4580.
34. Heo, J., Thapar, R., and Campbell, S. L. (2005) Recognition And Activation Of Rho GTPases By Vav1 And Vav2 Guanine Nucleotide Exchange Factors, *Biochemistry 44*, 6573−6585.
35. Bradford, M. M. (1976) A Rapid and Sensitive Method for the Quantitation of Microgram Quantities of Protein Utilizing the Principle of Protein-Dye Binding, *Anal. Biochem. 72*, 248−254.
36. Riener, C. K., Kada, G., and Gruber, H. J. (2002) Quick measurement of protein sulfhydryls with Ellman's reagent and with 4,4′-dithiodipyridine, *Anal. Bioanal. Chem. 373*, 266−276.
37. Hemsath, L., and Ahmadian, M. R. (2005) Fluorescence approaches for monitoring interactions of Rho GTPases with nucleotides, regulators, and effectors, *Methods 37*, 173−182.
38. Segel, I. H. (1993) *Enzyme kinetics*, Wiley-Interscience, New York.
39. Zhang, B., Zhang, Y., Wang, Z., and Zheng, Y. (2000) The role of Mg2+ cofactor in the guanine nucleotide exchange and GTP hydrolysis reactions of Rho family GTP-binding proteins, *J. Biol. Chem. 275*, 25299−25307.
40. Lenzen, C., Cool, R. H., and Wittinghofer, A. (1995) Analysis of intrinsic and CDC25-stimulated guanine nucleotide exchange of p21ras-nucleotide complexes by fluorescence measurements, *Methods Enzymol. 255*, 95−109.
41. Self, A. J., and Hall, A. (1995) Purification of recombinant Rho/Rac/G25K from Escherichia coli, *Methods Enzymol. 256*, 3−10.
42. Adams, P. D., Loh, A. P., and Oswald, R. E. (2004) Backbone dynamics of an oncogenic mutant of Cdc42Hs shows increased flexibility at the nucleotide-binding site, *Biochemistry 43*, 9968−9977.
43. Nimnual, A. S., Taylor, L. J., and Bar-Sagi, D. (2003) Redox-dependent downregulation of Rho by Rac, *Nat. Cell Biol. 5*, 236−241.
44. Joneson, T., and Bar-Sagi, D. (1998) A Rac1 effector site controlling mitogenesis through superoxide production, *J. Biol. Chem. 273*, 17991−17994.
45. Rikitake, Y., Kim, H. H., Huang, Z., Seto, M., Yano, K., Asano, T., Moskowitz, M. A., and Liao, J. K. (2005) Inhibition of Rho kinase (ROCK) leads to increased cerebral blood flow and stroke protection, *Stroke 36*, 2251−2257.
46. Rikitake, Y., and Liao, J. K. (2005) Rho GTPases, statins, and nitric oxide, *Circ. Res. 97*, 1232−1235.
47. Laufs, U., and Liao, J. K. (1998) Post-transcriptional regulation of endothelial nitric oxide synthase mRNA stability by Rho GTPase, *J. Biol. Chem. 273*, 24266−24271.
48. Laufs, U., Endres, M., Stagliano, N., Amin-Hanjani, S., Chui, D. S., Yang, S. X., Simoncini, T., Yamada, M., Rabkin, E., Allen, P. G., Huang, P. L., Bohm, M., Schoen, F. J., Moskowitz, M. A., and Liao, J. K. (2000) Neuroprotection mediated by changes in the endothelial actin cytoskeleton, *J. Clin. Invest. 106*, 15−24.
49. Shiga, N., Hirano, K., Hirano, M., Nishimura, J., Nawata, H., and Kanaide, H. (2005) Long-term inhibition of RhoA attenuates vascular contractility by enhancing endothelial NO production in an intact rabbit mesenteric artery, *Circ. Res. 96*, 1014−1021.
50. Kureishi, Y., Luo, Z., Shiojima, I., Bialik, A., Fulton, D., Lefer, D. J., Sessa, W. C., and Walsh, K. (2000) The HMG-CoA reductase inhibitor simvastatin activates the protein kinase Akt and promotes angiogenesis in normocholesterolemic animals, *Nat. Med. 6*, 1004−1010.
51. Wolfrum, S., Dendorfer, A., Rikitake, Y., Stalker, T. J., Gong, Y., Scalia, R., Dominiak, P., and Liao, J. K. (2004) Inhibition of Rho-kinase leads to rapid activation of phosphatidylinositol 3-kinase/protein kinase Akt and cardiovascular protection, *Arterioscler. Thromb. Vasc. Biol. 24*, 1842−1847.
52. Li, Z., Dong, X., Wang, Z., Liu, W., Deng, N., Ding, Y., Tang, L., Hla, T., Zeng, R., Li, L., and Wu, D. (2005) Regulation of PTEN by Rho small GTPases, *Nat. Cell Biol. 7*, 399−404.
53. Heo, J., Prutzman, K. C., Mocanu, V., and Campbell, S. L. (2005) Mechanism of Free Radical Nitric Oxide-mediated Ras Guanine Nucleotide Dissociation, *J. Mol. Biol. 346*, 1423−1440.
54. Heo, J., and Campbell, S. L. (2006) Ras Regulation by Reactive Oxygen and Nitrogen Species, *Biochemistry 45*, 2200−2210.
55. Ford, E., Hughes, M., and Wardman, P. (2002) Kinetics of the reactions of nitrogen dioxide with glutathione, cysteine, and uric acid at physiological pH, *Free Radical Biol. Med. 32*, 1314−1323.
56. Lenzen, C., Cool, R. H., Prinz, H., Kuhlmann, J., and Wittinghofer, A. (1998) Kinetic Analysis by Fluorescence of the Interaction between Ras and the Catalytic Domain of the Guanine Nucleotide Exchange Factor $Cdc25^{Mm}$, *Biochemistry 37*, 7420−7430.
57. Rossman, K. L., Der, C. J., and Sondek, J. (2005) GEF means go: turning on RHO GTPases with guanine nucleotide-exchange factors, *Nat. Rev. Mol. Cell Biol. 6*, 167−180.
58. Zhang, J., and Matthews, C. R. (1998) Ligand binding is the principal determinant of stability for the p21(H)-ras protein, *Biochemistry 37*, 14881−14890.

BI0610101